IEEE Access
Multidisciplinary | Rapid Review | Open Access Journal

Received June 23, 2020, accepted June 30, 2020, date of publication July 13, 2020, date of current version July 28, 2020.

Digital Object Identifier 10.1109/ACCESS.2020.3008895

A Novel Charging Algorithm for Lithium-Ion Batteries Based on Enumeration-Based Model Predictive Control

HUNG-YU PAI, GUAN-JHU CHEN, (Student Member, IEEE), YI-HUA LIU, (Member, IEEE), AND KUN-CHE HO

Department of Electrical Engineering, National Taiwan University of Science and Technology (NTUST), Taipei 106, Taiwan

Corresponding author: Yi-Hua Liu (yhliu@mail.ntust.edu.tw)

ABSTRACT Lithium-ion (Li-ion) batteries play a substantial role in energy storage solutions for modern-day technologies such as hand-held consumer electronics, aerospace, electric vehicles, and renewable energy systems. For Li-ion batteries, designing a high-quality battery charging algorithm is essential since it has significant influences on the performance and lifetime of Li-ion batteries. The objectives of a high-performance charger include high charging efficiency, short charging time, and long cycle life. In this paper, a model predictive control based charging algorithm is proposed, the presented technique aims to simultaneously reduce the charging time, and the temperature rise during charging. In this study, the coulomb counting method is utilized to calculate the future state-of-charge and an artificial neural network trained by experimental data is also applied to predict the future temperature rise. Comparing with the widely employed constant current-constant voltage charging method, the proposed charging technique can improve the charging time and the average temperature rise by 1.2 % and 4.13 %, respectively.

INDEX TERMS Model predictive control, artificial neural network, lithium-ion battery.

I. INTRODUCTION

Recently, the rapid development of electric vehicles and portable consumer devices has driven further advances in the technology of rechargeable batteries. Among the numerous types of rechargeable batteries, Lithium-ion (Li-ion) batteries featuring high energy density, more cycling lifetime, low self-discharge rate, and no memory effect have been widely applied in a variety of applications. From low power consumer electronics products to the high power storage system for stabilizing the renewable energy power generation, techniques related to Li-ion batteries have attracted lots of attention in the field of power electronics and power systems. To extract the maximum benefits from Li-ion battery, many types of research have focused on charging strategy. The most well-known conventional charging strategy is the constant current-constant voltage (CC-CV) charging method. In the CC-CV method, there is a constant current set to charge the battery cell until the cell voltage reaches an upper voltage limit. Next, a constant voltage is set to continue charging until the charging current decreases to the threshold value. The CC-CV method is simple to implement; however, there are issues of high-temperature rise derived by a large charging current at the CC stage, and long charging time problem caused by the CV stage. Other commonly adopted charging algorithms include pule charging techniques and multi-stage constant current (MSCC) charging methods.

In general, a charging strategy is evaluated by the charging efficiency, temperature rise, charging time, and its effect on the battery cycle life. In fact, it is difficult for a charging technique to improve all of the charging performances simultaneously. To some extent, they are in a trade-off relationship, i.e. a large charging current can shorten the charging time, but more power loss may arise along with the rapid temperature rise. To enhance the charging performances and make a good balance between charging time and charging losses, many studies have been proposed. They can be categorized into three groups, which are (i) CC-CV-based methods [1]–[4] (ii) pulse charging-based methods [5]–[11] and (iii) MSCC-based methods [12]–[19]. For category 1, ref. [1] proposed a fuzzy controller to allow more charging capacity at the CV stage with the consideration of open-circuit voltage.

The associate editor coordinating the review of this manuscript and approving it for publication was Yongquan Sun.

To generate a charging trajectory similar to the CC-CV method, authors in [2] developed a double loops control without the requirement of the current measurement. Likely, authors in [3] implemented phase-locked loop control and adjust the charging current appropriately using the phase angle as a control variable. Furthermore, the current pumped charger developed in [4] utilized the pumped charging current as in the CC stage and then used pulse current as in the CV stage, which takes a similar time but reaches a higher efficiency compared with conventional CC-CV method. For category 2, different settings of current value, pulse width, and pause time enable plenty of combinations of charging configurations. To speed up the charging process and improve the charging efficiency, the frequency and duty cycle of the constant voltage charging pulse were adjusted in [5]–[7] and [8], respectively. An adaptive pulse charging method proposed in [9] was able to obtain the same effect. Reference [10] employed a model-based optimization technique integrated with a second-order RC model to realize a pulse-amplitude-modulated charging method and a pulse-width-modulated charging method. In [11], temperature rise and the slope of the temperature rise were taken as inputs of a fuzzy controller to determine a proper charging current. Thus, the charging efficiency was improved due to the restricted temperature rise. For category 3, MSCC method adjusted the charging current value for different charging stages, so that it is capable of improving charging performance with more flexibility. But the determination of the individual current value and the criteria of transitions between stages turns out to be a challenge. The setting value of the charging current for each stage is very important since it has a great impact on the overall charging performance. Researchers have applied soft computing and design of experiments techniques to search for the optimal charging current value, including orthogonal array [12], Taguchi method [13]–[15], particle swarm optimization [16], and ant colony optimization [17]…etc. However, most of them are very time-consuming. Thus, ref. [18] formulated an equation that enables the determination of the optimal charging current value in an efficient way. Also, ref. [19] obtained optimal charging currents for the MSCC charging method based on Integer Linear Programming, which reduces the searching time for the optimal current.

As fast charging is becoming more desirable regardless of the applications and products, a large charging current is commonly used to shorten the charging time. However, the benefit of time reduction with a large charging current is usually followed by the issues of high temperature rise and increased power loss. More significantly, the negative effect on battery life and even safety concerns may arise at the same time [20]–[24]. Therefore, it is crucial to propose a charging strategy to optimize multiple objectives such as temperature rise and charging time to achieve the improvement of overall cycling performance.

Model predictive control (MPC) appears to be the most used optimization-based methodology for charging of Li-ion batteries [25]–[29]. MPC is selected due to its robustness and adaptability. Also, it can control multivariable nonlinear systems while takes an objective function and constraints on both inputs and states into account. In the context of Li-ion battery charging, MPC aims to optimize multiple objectives such as charging time, temperature rise, and state of health. In particular, ref. [25] has proposed MPC strategies based on pseudo-two-dimension (P2D) electrochemical model, while the works in [26]–[29] have suggested the use of reduced-order electrochemical models to simplify model complexity. For MPC configurations, most of the research in this area utilizes general MPC with the exception of [28] which is based on the sensitivity-based MPC and [29] which adopts nonlinear MPC. Using these approaches, the best control sequence can be analytically obtained by solving quadratic programming or Diophantine equations. However, the computation burden is high for these control schemes. Consequently, personal computer equips with advanced software such as MATLAB with optimization toolbox is typically required. Therefore, all the aforementioned papers provide only simulation results [25]–[29] or hardware-in-the-loop experiment results [29].

This paper proposes a novel charging method to reduce both charging time and temperature rise simultaneously. It should be noted that charging the Li-ion battery at low temperatures is likely to trigger lithium plating, which often leads to severe capacity fade. Consequently, preheating batteries from extremely low temperatures to a pre-defined temperature using the heat generated during charging may become thermodynamically favorable [30]. Therefore, the target application of the proposed charging technique is for Li-ion batteries operating in normal temperature range. Firstly, a temperature rise model based on artificial neural network (ANN) is built for the target battery cell. The proposed ANN can alleviate the complexity of electrochemical models by taking only input-output descriptions into account. Then, enumeration-based MPC is applied to determine the best charging current values for the next three sampling times. Enumeration-based MPC provides a straightforward approach to solve the optimization problem efficiently comparing with conventional MPC. Therefore, the computational cost can be reduced, which allows for the real-time implementation using low-cost microcontrollers. The main contribution of this study is the realization of the adaptive charging control based on enumeration-based MPC without the requirement of an accurate battery equivalent model, and an efficient way to simultaneously improve charging time and charging losses. To the best of our knowledge, this is the first time that such an approach is used in the context of the Li-ion battery charging. The experimental results validate that the proposed method can reduce the charging time and average temperature rise by 1.2% and 4.13%. comparing with the conventional CC-CV method.

II. METHODOLOGY

Fig. 1 shows a block diagram of the proposed charging strategy. An ANN model of temperature rise is built and trained in

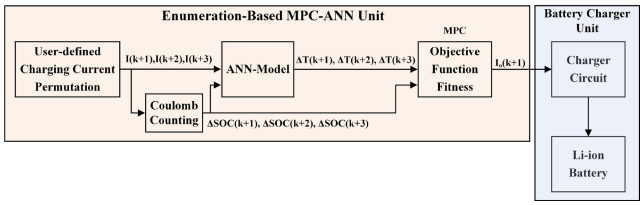

FIGURE 1. Block diagram of the proposed charging strategy.

advance. In this way, temperature rise can be calculated using the ANN model according to the inputted charging current and state of charge (SOC). Then, MPC is implemented to realize the on-line optimization of charging current based on instantaneous SOC which is estimated by the coulomb counting method and temperature rise value obtained from the trained ANN model. In this section, the temperature rise model based on ANN will be introduced, including the neural network design, data collection, and training as well as validation. In addition, implementation of the enumeration-based MPC and design of the objective function will be explained.

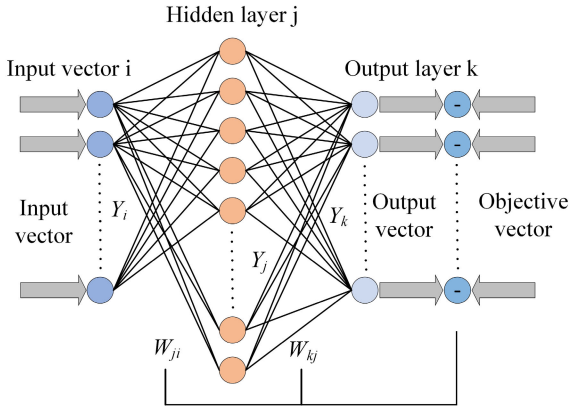

FIGURE 2. The structure of a backpropagation artificial neural network.

A. DESIGN AND IMPLEMENTATION OF THE NEURAL NETWORK MODEL

ANN is an algorithm inspired by biological neural systems. It has the capability of performing similar behavior of statistical methods such as regression, clustering, and classification. Moreover, its adaptability makes it particularly suitable for a system where the behavior is difficult to model or for a system lacks a mathematical model. Fig. 2 shows a typical backpropagation ANN. It is composed of several layers, including the input layer, hidden layer, and output layer. The layers consist of nodes, also known as "neuron". A node is regarded as a computation unit as given in Fig. 3. There are weightings connected between nodes, which determines which input signal and to what degree of the input signal should progress through the network to affect the outcome. To recognize the underlying relationship between input and output, "training" based on the database is needed. The training of ANN implies a continuous update of weightings and biases until training data consistently yield corresponding

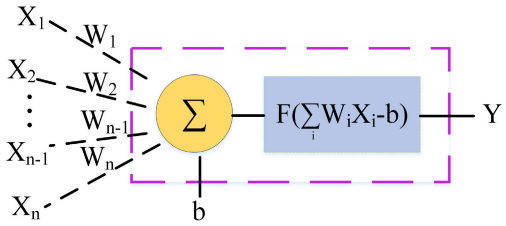

FIGURE 3. A mathematical model for artificial neuron.

outputs. The mathematical model of a node can be formulated as in (1) [31], [32].

$$Y = F(\sum_i W_i X_i - b) \tag{1}$$

where X is the input of a neuron, W is weighting, b is the bias, F is activation function and Y is the output of a neuron. The weighted inputs $W.X$ are added with a bias b. Then, the weighted summation passes through the activation function F, which ensures the unbounded input to turn into an output scaled in a certain range. Eventually, the desired output Y can be obtained.

The structure of an ANN consists of plenty of interconnections between nodes. In the input layer, the number of input neurons is dependent on the number of inputs of training data. In the middle is the hidden layer. The hidden layer can be single or multiple layers and it enables the representation of the nonlinear relationship between input and output. In fact, it is difficult to summarize the design process for the hidden layer with a few simple rules. The number of the hidden layer is associated with the complexity of the problem itself. Similar to the input layer, the number of output neurons for the output layer is determined by the numbers of the predicted target. There is no general designing rule that can be applied to determine the network topology for all situations; hence, it is typically determined by experience. Therefore, the selection of ANN network topology can be divided into two categories. The first type is to select a larger network first and remove redundant connections or nodes gradually through the experimental verifications. The second type is to select a smaller network first and expand the required connections and nodes. In this paper, the first type is adopted. If the training is completed, and the data is sufficient. The output can then be properly generated with any reasonable experimental data and values.

Fig. 4 shows the structure of the proposed ANN model for temperature rise estimation. There are four layers, including one input layer, two hidden layers, and one output layer. The battery charging current and SOC are taken as input parameters for the ANN model and the desired output is temperature rise. There are 35 nodes in the individual hidden layer. Tansig function shown in (2) is used as the activation function and training algorithm Trainlm (Levenberg - Marquardt) is applied in this study.

$$y(n) = \frac{e^n - e^{-n}}{e^n + e^{-n}} = \text{Tansig}(n) \tag{2}$$

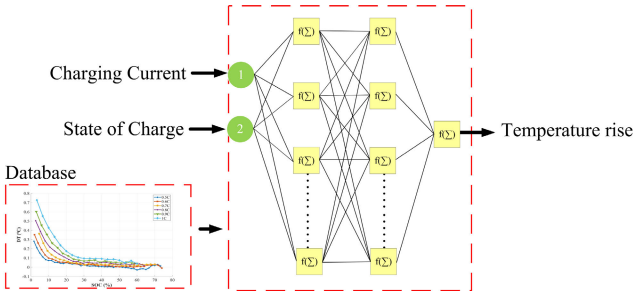

FIGURE 4. The proposed ANN structure for the temperature rise prediction.

Moreover, it is noted that the training data has a significant effect on the performance of the ANN for accurately predicting the desired output. The collection procedure of the training data is described as below:

TABLE 1. Database for ANN model for training.

Number of training data set					
0.5C	0.6C	0.7C	0.8C	0.9C	1.0C
84	64	52	43	35	29

TABLE 2. Database for ANN model for validation.

Number of the validation data set					
0.5C	0.6C	0.7C	0.8C	0.9C	1.0C
4	4	4	4	4	4

Firstly, the battery cell is discharged using 0.2 C until the open-circuit voltage (OCV) reaches its lower limit. Then, to acquire the temperature rise under different charging currents, 6 charging currents ranging from 0.5 C to 1.0 C with the interval of 0.1 C are set to charge the battery cell as given in Table 1 and Table 2. In this paper, the utilized battery is the NCR18650B Li-ion battery manufactured by PANASONIC corp. The battery specifications are shown in Table 3. In this study, the tested battery cell is located in the isothermal chamber to ensure the ambient temperature always kept at 25 °C. The surface temperature is recorded with the sampling time of 2 minutes during the entire constant current charging period. In this way, there are 331 data sets obtained in total. Among them, 307 data sets are for training while 24 data sets are for validation. It should be noted that the charging time varies with the charging currents. Thus, the total number of the data points for 6 charging conditions are different from each other due to the fixed sampling time. Eventually, the training data is composed of two input vectors for SOC and charging C-rate with the size of [1 × 307] and an output target vector for temperature rise with the size of [1 × 307]. Fig. 5 shows the training data in the plot of temperature rise versus SOC under different charging currents. In Fig. 5, the temperature rise is defined as the difference between the surface temperature and the ambient temperature. From Fig. 5, high temperature rise can be observed at low SOC due to the fact that the total heat generation inside the battery includes reversible entropic heat and joule heat loss, while the latter is a function of the battery internal resistance and the charging current. Since the heat generation is proportional to internal

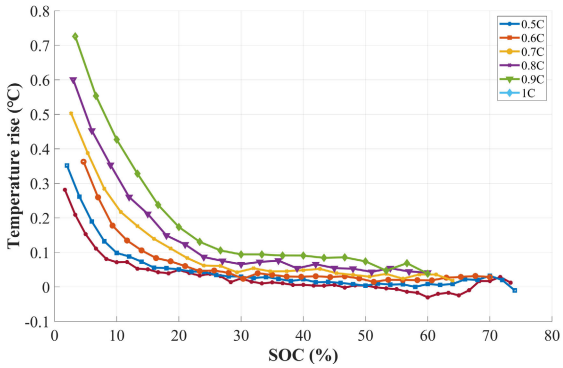

FIGURE 5. Temperature rise versus SOC under different charging current.

TABLE 3. NCR18650B specifications [33].

PANASONIC NCR18650B Li-Ion Battery	
Nominal Capacity	3350 mAh
Nominal Voltage	3.6V
Cut-off Voltage	2.5 V
Standard Charge	CC-CV，1625 mA，4.2 V
Dimension	18.5 mm (diameter)，63 mm (height)
Weight	48.5 g
Charge Temperature	0 °C to +45 °C
Discharge Temperature	-20 °C to +60 °C

resistance; hence, high resistance at low SOC will result in high temperature loss.

In this paper, the implementation of proposed backpropagation ANN, as well as the training and validation, are realized by MATLAB software. The predicted output is evaluated by calculating the mean squared error. After the completion of the ANN training, 24 sets of data that are distributed uniformly in the overall data set are inputted to the trained ANN model to validate the accuracy of the obtained ANN. Fig. 6 shows the error between the predicted result and the actual measured value. It can be observed that the maximum error of temperature rise is 0.05°C, which is acceptable for modeling the temperature behavior of the battery cell.

B. THE PROPOSED ENUMERATION-BASED MPC

Model predictive control had been broadly applied in the nonlinear and time-variant system in the industry due to the advantages of high robustness and adaptability [34]. Especially, MPC allows the current timeslot to be optimized, while takes future timeslot into account. Fig. 7 shows the basic concept of an MPC where k represents sampling time, u is input, y is past output, $\hat{y}$ is predicted output, and P is the length of the prediction steps. The error between target and output $\hat{y}$ is evaluated by objective function and then optimized to determine the control command for the next step [35].

In this paper, the enumeration-based MPC method is used to determine the control parameters, namely the value of the charging current for the next three sampling time sequence. Enumeration-based MPC is applied hereby due to its superiority of moderate computational complexity and simplicity [36]. Based on the trained ANN model and

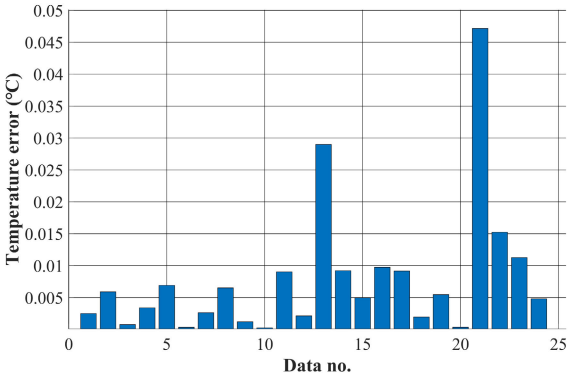

FIGURE 6. Validation results of the proposed ANN model.

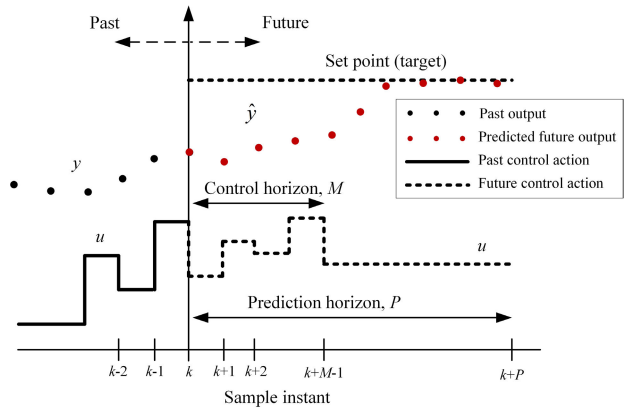

FIGURE 7. Response plot of a model predictive control'.

coulomb counting, the performance (temperature rise and SOC) of all possible control sequences derived from MPC can be obtained, and then evaluated by the objective function. To realize an optimal charging strategy where more capacity can be charged with less temperature rise, the objective function is design as given in (3). In this way, the result is evaluated by considering both the increment of SOC and the temperature rise, i.e. ΔSOC and ΔT, respectively. Also, the importance of these two terms can be adjusted by the weighting factor α. In this paper, two objective functions with different weighting factors are investigated. They are (i) MPC-ANN: a fixed weighting factor with $\alpha = 0.65$ and (ii) MPC-ANN-VW: the weighting factor is varied with the charging current as given in (4).

$$J = \alpha \sum_{i=1}^{3} \left(\frac{SOC_{\max} - SOC(i)}{SOC_{\max}} \right) + (1-\alpha) \sum_{i=1}^{3} \frac{DT(i)}{DT_{\max}} \quad (3)$$

where J is the fitness value, α is weighting factor, $SOC(i)$ is SOC at the time step i, SOC_{max} is the maximum SOC for all possible control sequences, $DT(i)$ is temperature rise at time step i, DT_{max} is maximum temperature rise for all possible control sequences.

$$\alpha = -1 \times I_{charge\_c-rate} + 1.5 \quad (4)$$

where I_{charge_c-rate} represents the charging current command in C-rate.

In Eq. (3), the first term represents the normalized charged capacity and the second term describes the normalized temperature rise value. By changing the value of α, the importance of both term can be adjusted. In Eq. (4), the weighting factor is inverse proportional to the charging current. For example, a high charging current ($I_{charge\_c-rate} = 1.0$ C) results in a low α value, which means the importance of temperature rise will be emphasized. On the other hand, a low charging current will highlight the importance of charged capacity.

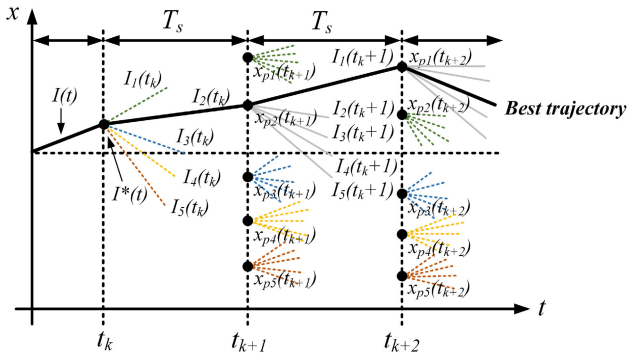

FIGURE 8. Conceptual diagram of the MPC with enumeration.

Fig. 8 shows the conceptual diagram of the proposed enumeration-based MPC method. When there are N possible settings of charging current in the next P time steps, the total possible combinations of the charging configurations will be NP. In this paper, the prediction is made for 3-time steps, and for each step, there are 5 settings of the charging current. In other words, N = 5 and P = 3. Hence, the proposed enumeration-based MPC has to deal with 125 combinations of the possible charging current sequences. Fig. 9 presents the flowchart of the proposed charging strategy. Firstly, SOC at the current time step is estimated by the coulomb counting approach. Next, based on the estimated SOC and 125 combinations of the charging current sequence derived from the enumeration, the ANN model can predict the temperature rise. Also, the charged capacity can be calculated. Then, both performance indexes, i.e. temperature rise and charged capacity, are normalized into a range of 0 to 1 for the current time step. The best charging sequence can then be obtained by finding the charging current sequence with minimal fitness value as shown in (3). Finally, the first element in the optimal charging current sequence is selected as the charging current command. The charging current keeps updating until the termination criterion is satisfied.

III. EXPERIMENTAL RESULTS

Fig. 10 shows the experimental platform utilized to realize and validate the proposed charging strategy. All the battery cells are in the isothermal chamber to ensure the ambient temperature always kept at 25 °C. Temperature is monitored using temperature acquisition tool USB NI 9211 and is plotted in the user-interface using LabView. Three charging

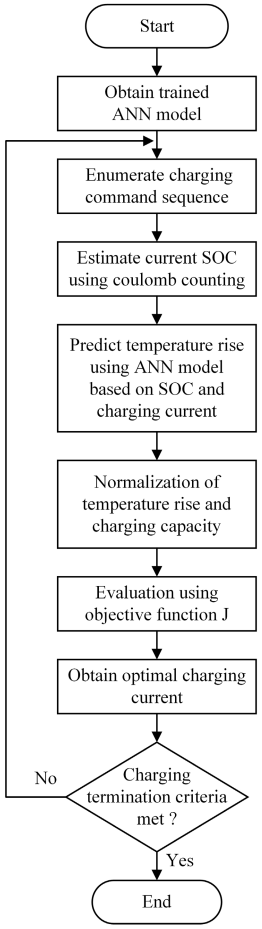

FIGURE 9. Flowchart of the proposed charging strategy.

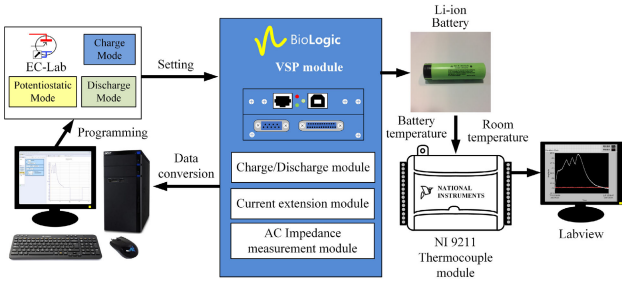

FIGURE 10. Experimental platform.

methods are implemented for comparison, including the conventional CC-CV method and the proposed charging strategy with two different objective functions, namely MPC-ANN and MPC-ANN-VW.

Fig. 11 and Fig. 12 shows the recorded voltage, current, and temperature rise data of MPC-ANN and MPC-ANN-VW, respectively. It can be observed that both charging currents decrease with the rising temperature. Moreover, the conventional CC-CV method with charging current ranging from 0.7 C to 1.0 C in the interval of 0.1 C is compared with the proposed methods. Fig. 13 shows the result of the temperature rise of each charging strategy. The overall charging performances are given in Table. 3, including charging time and the

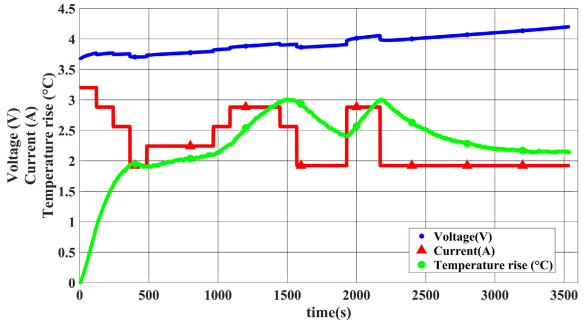

FIGURE 11. Voltage, current and temperature log data of MPC-ANN.

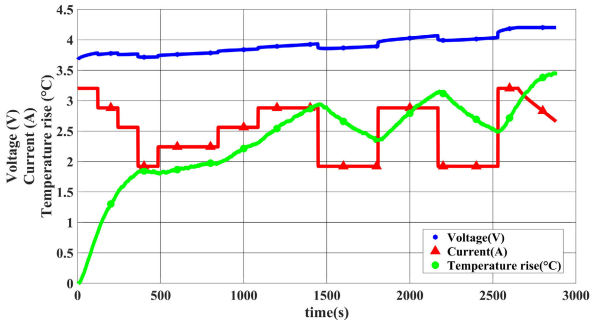

FIGURE 12. Voltage, current and temperature log data of MPC-ANN-VW.

average temperature rise during the charging process. Due to different charging currents, the resulted charging time varied from each other. To compare temperature rise fairly, two indicators are defined. The average temperature rise, denoted as AVG1, is calculated by (5) where $t_{end,i}$ is the charging time of method *i*. AVG1 can be regarded as the average temperature rise over the whole period of the charging method itself. On the other hand, the average temperature rise in a specific time interval, denoted as AVG2, is defined as (6), where $t_{end,cccv}$ is the charging time of the 1C CC-CV method. AVG2 represents the comparison based on the same time interval with the 1C CC-CV method, i.e. the average temperature rise within 6103 seconds.

$$\mathrm{AVG1} = \frac{\int_0^{t_{end},i} \Delta T(t)dt}{t_{end},i} \tag{5}$$

$$\mathrm{AVG2} = \frac{\int_0^{t_{end},CCCV} \Delta T(t)dt}{t_{end},CC-CV} \tag{6}$$

According to Table 4, a larger charging current results in shorter charging time but increases the temperature rise. It can also be observed that the performance of the proposed charging strategy is close to the ones using 0.7 C and 0.8 C CC-CV method. Thus, an additional experiment of 0.75 C CC-CV is carried out for comparison. It can be seen from Table 5 that MPC-ANN has the best AVG1 value while MPC-ANN-VW has the best AVG2 value. Tables 5 and 6 show the improvement of MPC-ANN and MPC-ANN-VW compared with the CC-CV method, respectively. From Table 5,

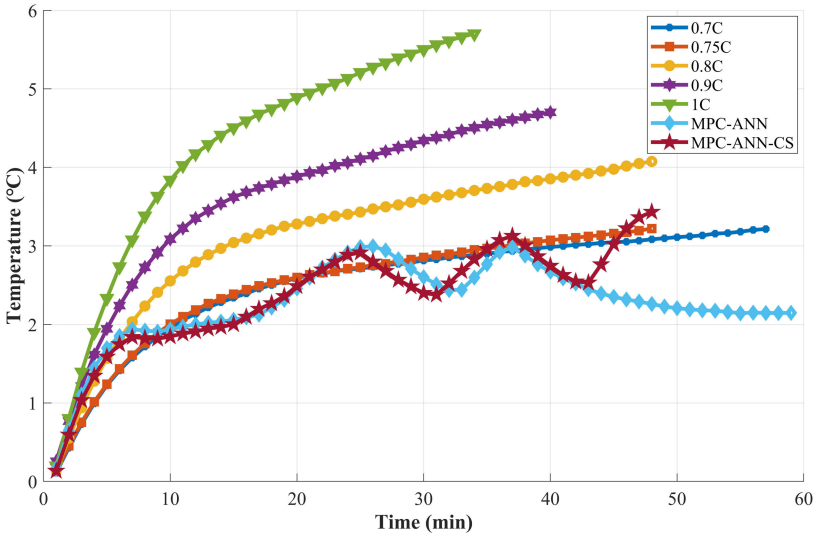

FIGURE 13. Comparison of the temperature rise of different charging strategies.

TABLE 4. Experimental result of CC-CV method, MPC-ANN, and MPC-ANN-VW.

Charging strategy	Charging time (s)	AVG1 (°C)	AVG2 (°C)
0.7C CC-CV	7022	2.54	2.18
0.75C CC-CV	6860	2.56	2.21
0.8C CC-CV	6616	3.10	2.80
0.9C CC-CV	6318	3.55	3.37
1C CC-CV	6103	4.21	4.21
MPC-ANN	6909	2.27	2.18
MPC-ANN-VW	6663	2.41	2.12

TABLE 5. Improvement of MPC-ANN compared with CC-CV method.

Charging strategy	Charging time (s)	AVG1	AVG2
0.7C CC-CV	1.61%	10.31%	0.22%
0.75C CC-CV	-2.45%	9.73%	1.61%
0.8C CC-CV	-4.43%	26.53%	22.10%
0.9C CC-CV	-9.35%	36.02%	35.32%
1C CC-CV	-13.21%	46.03%	48.33%

MPC-ANN shows the improvement on AVG1 and AVG2 by 9.73%, 1.61%, while the time consumption is increased by 2.45% compared with 0.75 C CC-CV method. From Table 6, MPC-ANN-VW shows the improvement of charging time, AVG1, and AVG2 by 1.2%, 4.34%, and 4.13% compared with 0.75C CC-CV method. In conclusion, MPC-ANN has better performance in temperature rise with the similar time consumption of 0.75C CC-CV method. On the other hand, MPC-ANN-VW shows a better balance between charging time and temperature rise.

IV. CONCLUSION

This paper proposes a novel charging strategy that combines the ANN model and MPC. Based on ANN, the temperature rise of the battery cell can be predicted. With the trained ANN model, enumeration-based MPC enables the optimization of the charging current. In this way, the temperature rise can be reduced during the charging process, which achieves the power loss reduction and thus prolongs battery lifetime. The highlights of the proposed charging strategy are:

- It can predict future battery states under any possible future charging sequence and hence evaluate charging performance over a prediction period.
- It calculates the best charging sequence using an optimization method, which can solve multi-objective problems.
- It utilizes a receding horizon strategy and only applies the first element of the best charging sequence at each control moment. The prediction error caused by model inaccuracy will not accumulate because instantaneous measurements correctly update each initial prediction value.

Besides, the design of the objective function is investigated with two different weighting factors. Compared with the 0.75 C CC-CV method, the MPC-ANN-VW method improves the charging time by 1.2%, and the average temperature rise by 4.13%. MPC-ANN method improves the average temperature rise by 9.73% but it requires 2.45% more charging time. Future directions of research will focus on the experimental validation of the cycle-life improvement

TABLE 6. Improvement of MPC-ANN-VW compared with CC-CV method.

Charging strategy	Charging time (s)	AVG1	AVG2
0.7C CC-CV	5.11%	4.95%	2.77%
0.75C CC-CV	1.20%	4.34%	4.13%
0.8C CC-CV	-0.71%	22.14%	24.10%
0.9C CC-CV	-5.46%	32.20%	36.97%
1C CC-CV	-9.18%	42.81%	49.66%

of the proposed method, and to investigate the possibility of generating training data of ANN using electrochemical models.

REFERENCES

[1] G.-C. Hsieh, L.-R. Chen, and K.-S. Huang, "Fuzzy-controlled Li-ion battery charge system with active state-of-charge controller," *IEEE Trans. Ind. Electron.*, vol. 48, no. 3, pp. 585–593, Jun. 2001.

[2] K. M. Tsang and W. L. Chan, "Current sensorless quick charger for lithium-ion batteries," *Energy Convers. Manage.*, vol. 52, no. 3, pp. 1593–1595, Mar. 2011.

[3] L.-R. Chen, "PLL-based battery charge circuit topology," *IEEE Trans. Ind. Electron.*, vol. 51, no. 6, pp. 1344–1346, Dec. 2004.

[4] L.-R. Chen, J.-J. Chen, N.-Y. Chu, and G.-Y. Han, "Current-pumped battery charger," *IEEE Trans. Ind. Electron.*, vol. 55, no. 6, pp. 2482–2488, Jun. 2008.

[5] L.-R. Chen, "A design of an optimal battery pulse charge system by frequency-varied technique," *IEEE Trans. Ind. Electron.*, vol. 54, no. 1, pp. 398–405, Feb. 2007.

[6] L.-R. Chen, "Design of duty-varied voltage pulse charger for improving Li-ion battery-charging response," *IEEE Trans. Ind. Electron.*, vol. 56, no. 2, pp. 480–487, Feb. 2009.

[7] P. de Jongh and P. H. L. Notten, "Effect of current pulses on lithium intercalation batteries," *Solid State Ionics*, vol. 148, nos. 3–4, pp. 259–268, Jun. 2002.

[8] J. Li, E. Murphy, J. Winnick, and P. A. Kohl, "The effects of pulse charging on cycling characteristics of commercial lithium-ion batteries," *J. Power Sources*, vol. 102, nos. 1–2, pp. 302–309, Dec. 2001.

[9] H. Fang, C. Depcik, and V. Lvovich, "Optimal pulse-modulated lithium-ion battery charging: Algorithms and simulation," *J. Energy Storage*, vol. 15, pp. 359–367, Feb. 2018.

[10] S. Sirisukprasert and S. M. I. Niroshana, "An adaptive pulse charging algorithm for lithium batteries," in *Proc. 14th Int. Conf. Electr. Eng./Electron., Comput., Telecommun. Inf. Technol. (ECTI-CON)*, Jun. 2017, pp. 218–221.

[11] S.-C. Wang, G.-J. Chen, and Y.-H. Liu, "Adaptive charging strategy with temperature rise mitigation and cycle life extension for Li-ion batteries," *CPSS Trans. Power Electron. Appl.*, vol. 3, no. 3, pp. 202–212, Sep. 2018.

[12] Y.-H. Liu, C.-H. Hsieh, and Y.-F. Luo, "Search for an optimal rapid charging pattern for li-ion batteries using consecutive orthogonal arrays," *IEEE Trans. Energy Convers.*, vol. 26, no. 2, pp. 654–661, Jun. 2011.

[13] T. T. Vo, X. Chen, W. Shen, J.-A. Jiang, and A. Kapoor, "New charging strategy for lithium-ion batteries based on the integration of Taguchi method and state of charge estimation," *J. Power Sources*, vol. 273, pp. 413–422, Jan. 2015.

[14] Y.-H. Liu and Y.-F. Luo, "Search for an optimal rapid-charging pattern for Li-ion batteries using the Taguchi approach," *IEEE Trans. Ind. Electron.*, vol. 57, no. 12, pp. 3963–3971, Dec. 2010.

[15] C.-H. Lee, M.-Y. Chen, S.-H. Hsu, and J.-A. Jiang, "Implementation of an SOC-based four-stage constant current charger for Li-ion batteries," *J. Energy Storage*, vol. 18, pp. 528–537, Aug. 2018.

[16] C.-H. Lee, T.-W. Chang, S.-H. Hsu, and J.-A. Jiang, "Taguchi-based PSO for searching an optimal four-stage charge pattern of Li-ion batteries," *J. Energy Storage*, vol. 21, pp. 301–309, Feb. 2019.

[17] Y.-H. Liu, J.-H. Teng, and Y.-C. Lin, "Search for an optimal rapid charging pattern for lithium-ion batteries using ant colony system algorithm," *IEEE Trans. Ind. Electron.*, vol. 52, no. 5, pp. 1328–1336, Oct. 2005.

[18] A. B. Khan and W. Choi, "Optimal charge pattern for the high-performance multistage constant current charge method for the Li-ion batteries," *IEEE Trans. Energy Convers.*, vol. 33, no. 3, pp. 1132–1140, Sep. 2018.

[19] L.-R. Dung and J.-H. Yen, "ILP-based algorithm for lithium-ion battery charging profile," in *Proc. IEEE Int. Symp. Ind. Electron.*, Jul. 2010, pp. 2286–2291.

[20] F. Leng, C. M. Tan, and M. Pecht, "Effect of temperature on the aging rate of Li ion battery operating above room temperature," *Sci. Rep.*, vol. 5, Aug. 2015, Art. no. 12967.

[21] C. Zhang, J. Jiang, Y. Gao, W. Zhang, Q. Liu, and X. Hu, "Charging optimization in lithium-ion batteries based on temperature rise and charge time," *Appl. Energy*, vol. 194, pp. 569–577, May 2017.

[22] L. Patnaik, A. V. J. S. Praneeth, and S. S. Williamson, "A closed-loop constant-temperature constant-voltage charging technique to reduce charge time of lithium-ion batteries," *IEEE Trans. Ind. Electron.*, vol. 66, no. 2, pp. 1059–1067, Feb. 2019.

[23] A. Aktas, "Design and implementation of adaptive battery charging method considering the battery temperature," *IET Circuits, Devices Syst.*, vol. 14, no. 1, pp. 72–79, Jan. 2020.

[24] Y. Gao, X. Zhang, B. Guo, C. Zhu, J. Wiedemann, L. Wang, and J. Cao, "Health-aware multiobjective optimal charging strategy with coupled electrochemical-thermal-aging model for lithium-ion battery," *IEEE Trans. Ind. Informat.*, vol. 16, no. 5, pp. 3417–3429, May 2020.

[25] M. Torchio, L. Magni, R. D. Braatz, and D. M. Raimondo, "Optimal health-aware charging protocol for lithium-ion batteries: A fast model predictive control approach," *IFAC-PapersOnLine*, vol. 49, no. 7, pp. 827–832, Aug. 2016.

[26] C. Zou, C. Manzie, and D. Nešić, "Model predictive control for lithium-ion battery optimal charging," *IEEE/ASME Trans. Mechatronics*, vol. 23, no. 2, pp. 947–957, Apr. 2018.

[27] R. Suresh and R. Rengaswamy, "Modeling and control of battery systems. Part II: A model predictive controller for optimal charging," *Comput. Chem. Eng.*, vol. 119, pp. 326–335, Nov. 2018.

[28] A. Pozzi, M. Torchio, D. R. Braatz, and M. D. Raimondo, "Optimal charging of an electric vehicle battery pack: A real-time sensitivity-based model predictive control approach," *J. Power Sources*, vol. 461, Jun. 2020, Art. no. 228133.

[29] Y. Yin and S.-Y. Choe, "Actively temperature controlled health-aware fast charging method for lithium-ion battery using nonlinear model predictive control," *Appl. Energy*, vol. 271, Aug. 2020, Art. no. 115232.

[30] X. Hu, Y. Zheng, D. A. Howey, H. Perez, A. Foley, and M. Pecht, "Battery warm-up methodologies at subzero temperatures for automotive applications: Recent advances and perspectives," *Prog. Energy Combustion Sci.*, vol. 77, Mar. 2020, Art. no. 100806.

[31] W. Sheng, P. Shan, J. Mao, Y. Zheng, S. Chen, and Z. Wang, "An adaptive memetic algorithm with rank-based mutation for artificial neural network Architecture optimization," *IEEE Access*, vol. 5, pp. 18895–18908, Sep. 2017.

[32] J.-H. Chang and C.-Y. Tseng, "Analysis of correlation between secondary PM2.5 and factory pollution sources by using ANN and the correlation coefficient," *IEEE Access*, vol. 5, pp. 22812–22822, Oct. 2017.

[33] *Lithium Ion Battery-NCR18650B*, Specification Report, Ver. 13.11 R1, Panasonic Inc., Kadoma, Japan, 2012.

[34] E.-S. Jun, S. Kwak, and T. Kim, "Performance comparison of model predictive control methods for active front end rectifiers," *IEEE Access*, vol. 6, pp. 77272–77288, Nov. 2018.

[35] S. V. Puranik, A. Keyhani, F. Khorrami, W. H. Jung, and S. H. Kim, "A vehicle trajectory tracking method with a time-varying model based on the model predictive control," *IEEE Access*, vol. 8, pp. 16573–16583, Dec. 2019.

[36] P. Karamanakos, T. Geyer, and S. Manias, "Direct voltage control of DC–DC boost converters using enumeration-based model predictive control," *IEEE Trans. Power Electron.*, vol. 29, no. 2, pp. 968–978, Feb. 2014.

HUNG-YU PAI was born in Changhua, Taiwan, in 1997. He received the B.S. degree in electrical engineering from the National Taiwan University of Science and Technology, in 2019, where he is currently pursuing the Ph.D. degree with the Department of Electrical Engineering. His research interests include power electronics, Li-ion battery charging algorithm, and Li-ion battery SOC estimation algorithm.

GUAN-JHU CHEN (Student Member, IEEE) was born in Taichung, Taiwan, in 1990. He received the B.S. degree in electrical engineering from Kun Shan University, in 2012, and the M.S. degree in electrical engineering from the National Taiwan University of Science and Technology (NTUST), in 2014, where he is currently pursuing the Ph.D. degree with the Department of Electrical Engineering. His research interests include power electronics, digital power control, and Li-ion battery charging algorithm.

YI-HUA LIU (Member, IEEE) received the Ph.D. degree in electrical engineering from National Taiwan University, Taipei, Taiwan, in 1998. He joined the Department of Electrical Engineering, Chang-Gung University, Taoyuan, Taiwan, in 2003. He is currently with the Department of Electrical Engineering, National Taiwan University of Science and Technology, Taipei. His current research interests include power electronics and battery management.

KUN-CHE HO was born in Taichung, Taiwan, in 1991. He received the bachelor's and master's degrees in electronic and computer engineering from the National Taiwan University of Science and Technology, Taipei, Taiwan, in 2015, where he is currently pursuing the Ph.D. degree with the Department of Electrical Engineering, with a focus on switch power supply, LED driver, and battery management.